

# Asymptotic Parachute Performance Sensitivity

David W. Way, Richard W. Powell, Allen Chen\*, Adam D. Steltzner\*

NASA Langley Research Center

1 North Dryden Street, Mail Stop 489

Hampton, VA 23681-2199

757-864-8149

David.W.Way@nasa.gov

\*Jet Propulsion Laboratory, Pasadena, CA

*Abstract*—In 2010, the Mars Science Laboratory mission will pioneer the next generation of robotic Entry, Descent, and Landing systems by delivering the largest and most capable rover to date to the surface of Mars. In addition to landing more mass than any other mission to Mars, Mars Science Laboratory will also provide scientists with unprecedented access to regions of Mars that have been previously unreachable. By providing an Entry, Descent, and Landing system capable of landing at altitudes as high as 2 km above the reference gravitational equipotential surface, or areoid, as defined by the Mars Orbiting Laser Altimeter program, Mars Science Laboratory will demonstrate sufficient performance to land on 83% of the planet's surface. By contrast, the highest altitude landing to date on Mars has been the Mars Exploration Rover at 1.3 km below the areoid. The coupling of this improved altitude performance with latitude limits as large as 60 degrees off of the equator and a precise delivery to within 10 km of a surface target, will allow the science community to select the Mars Science Laboratory landing site from thousands of scientifically interesting possibilities.

In meeting these requirements, Mars Science Laboratory is extending the limits of the Entry, Descent, and Landing technologies qualified by the Mars Viking, Mars Pathfinder, and Mars Exploration Rover missions. Specifically, the drag deceleration provided by a Viking-heritage 16.15 m supersonic Disk-Gap-Band parachute in the thin atmosphere of Mars is insufficient, at the altitudes and ballistic coefficients under consideration by the Mars Science Laboratory project, to maintain necessary altitude performance and timeline margin. This paper defines and discusses the asymptotic parachute performance observed in Monte Carlo simulation and performance analysis and its effect on the Mars Science Laboratory Entry, Descent, and Landing architecture.<sup>1,2</sup>

<sup>1</sup> U.S. Government work not protected by U.S. copyright.

<sup>2</sup> IEEEAC paper #1465.

## TABLE OF CONTENTS

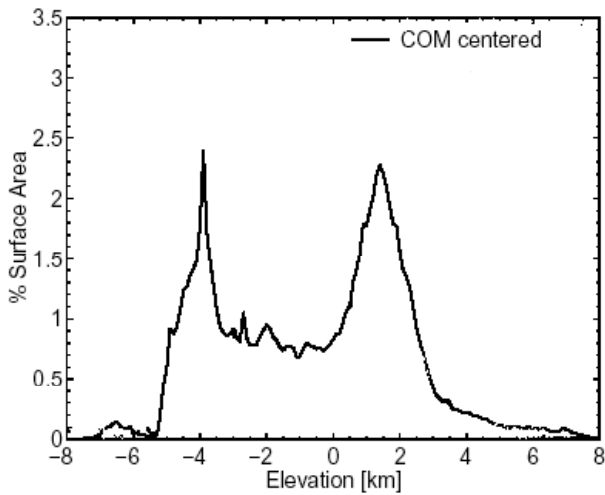
<b>1. INTRODUCTION</b> .....	<b>1</b>
<b>2. EDL SEQUENCE OF EVENTS</b> .....	<b>2</b>
<b>3. MOTIVATION</b> .....	<b>4</b>
<b>4. DEVELOPMENT</b> .....	<b>4</b>
<b>5. SIMULATION RESULTS</b> .....	<b>5</b>
<b>6. SUMMARY</b> .....	<b>8</b>
<b>ACKNOWLEDGEMENTS</b> .....	<b>9</b>
<b>REFERENCES</b> .....	<b>9</b>
<b>BIOGRAPHY</b> .....	<b>9</b>

## 1. INTRODUCTION

Mars Science Laboratory (MSL), expected to launch in 2009, will be the next generation rover in robotic exploration of Mars. Building on the success of the twin Mars Exploration Rover (MER) rovers, *Spirit* and *Opportunity*, which landed in 2004, MSL will collect Martian soil samples and rock cores and analyze them for organic compounds and environmental conditions that could support life now or could have supported life in the past.

The MSL Entry, Descent, and Landing (EDL) architecture is driven by a need to land the largest scientific payload, a 775 kg rover, to the highest altitude, 2.0 km above the Mars Orbiting Laser Altimeter (MOLA) defined areoid, with the highest precision, less than 10 km, of any previous mission to Mars. The motivation for these driving EDL requirements is to allow the scientific community to select the MSL landing site from the largest possible set of safe landing sites in order to place the rover in a location with the highest probability of achieving the science objectives. The hypsometric curve of Mars, Figure 1, shows that nearly 83% of the Martian terrain lies at elevations within the MSL altitude capability of 2.0 km. Starting in 2006, a set of site selection meetings will be conducted which are open to public participation and are anticipated to involve scientists from around the country. The planned process follows

closely the process used for selecting the two landing sites



for the Mars Exploration Rovers [Ref 1].

**Figure 1 – hypsometric curve of Mars.**

To date, the United States has performed five successful landings on Mars, Viking Lander I (20-July-1976), Viking Lander II (3-September-1976), Mars Pathfinder (4-July-1997), MER-A (3-January-2004), and MER-B (24-January-2004). An additional landed mission, Phoenix, will occur before MSL is launched and is scheduled for launch in 2007. These missions, compared in Table 1, form the core EDL heritage technologies on which MSL heavily relies. The MSL EDL design team has constructed an EDL architecture that leverages these proven technologies wherever possible and combines them with novel innovations in order to extend the performance envelope to the maximum extent possible.

**Table 1 – Comparison to Previous Missions.**

Parameter	Viking	MPF	MER	Phoenix	MSL
Entry Mass (kg)	980	585	836	603	2804
Landed Mass (kg)	612	370	539	364	1591
Mobile Mass (kg)	0	11	173	0	775
Landing Site Altitude (km)	-3.5	-1.5	-1.3	-3.5	+2.0

The project has conducted analysis that demonstrates that the MSL EDL architecture will meet the performance requirements consistent with delivering a 775 kg rover to 2 km MOLA in a 10 km ellipse.

## 2. EDL SEQUENCE OF EVENTS

The following section briefly describes the MSL EDL sequence. Details of the MSL EDL architecture may be found in [Ref 2]. For the purposes of this paper, EDL is defined to begin at Cruise Stage separation and ends with Descent Stage flyaway. Deceleration during EDL is achieved through a combination of a 70-degree sphere-cone aeroshell flown at an angle-of-attack to generate lift as well as drag; a supersonically deployed Disk-Gap-Band (DGB) parachute; and Viking-derived monopropellant liquid rocket engines. Final touchdown with the surface is made directly on the rover mobility system in a novel “Sky Crane” maneuver. This paper will focus on vehicle flight mechanics while on the parachute between Supersonic Parachute (SSP) deploy and heatshield jettison.

### *Cruise Stage Separation and Turn to Entry*

EDL begins approximately 10 minutes prior to atmospheric entry interface when the entry vehicle separates from the Cruise Stage. Attitude determination is performed during cruise using a star scanner. Prior to Cruise Stage separation, the current navigation state is uploaded to the flight computer. Assumptions in modeling the potential errors in this attitude initialization have a pronounced effect in the simulated EDL performance.

### *Atmospheric Entry and Hypersonic Aeromanuevering*

Entry interface occurs at a defined radius of 3522.2 km and marks the beginning of the entry phase. Objectives during the entry phase are to survive the entry environment, including the aeroheating heat pulse and structural g-loading, and arrive at the desired supersonic parachute deploy target by using vehicle lift to compensate for dispersions in initial delivery state, atmosphere, and aerodynamics [Ref 3].

Lifting entries provide several advantages over ballistic entries. Using lift to adjust drag acceleration allows control of the range flown, significantly reducing the landing footprint ellipse. Using lift also allows a significant increase in the supersonic parachute deploy altitude and thus the landing site elevation capability.

Aerodynamic lift is generated by a center-of-gravity offset from the vehicle axis of symmetry, which causes the aeroshell to fly at a non-zero trim angle-of-attack. The current baseline configuration, Figure 2, provides for a hypersonic lift-to-drag ratio (L/D) of 0.24 by means of a tungsten mass attached to the backshell at the heatshield separation plane.

typically selected to achieve a nominal jettison at Mach 0.7, allowing +/- 0.1 in Mach number for dispersions.

### *Terminal Descent Initiation and Powered Approach*

There are two functions involved in the determination of when to start powered descent. First, the navigation Filter must process the TDS measurements and estimate the spacecraft ground-relative velocity vector and altitude above the terrain. Second, the powered descent guidance must evaluate the altitude and velocity and determine a solution for the time to initiate the powered descent sequence.

The TDS is required to update the navigated altitude and velocity to acceptable levels prior to initiating the terminal descent. It is the available time in this configuration, in which the terminal descent guidance is processing TDS data prior to the initiation of powered descent, which provides and indicator of the degree of timeline margin in the system.

Terminal descent initiation begins with Mars Lander Engine (MLE) catalyst bed warm-up, prior to release of the backshell and parachute. After warm-up, the Descent Stage separates from the backshell and Guidance, Navigation, and Control algorithms take active control of the MLE throttles to maintain vehicle attitude and deliver the spacecraft to a predetermined Sky Crane waypoint with near-zero horizontal velocity.

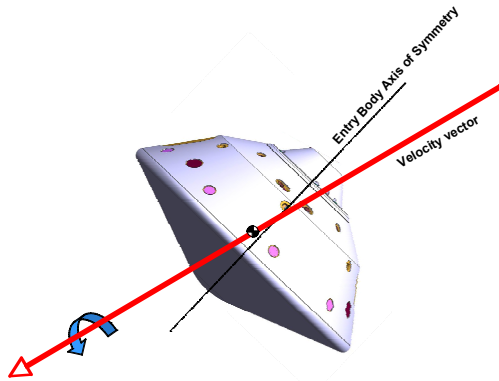


**Figure 2 – Entry Vehicle.**

### *Supersonic Parachute Deployment and Parachute Descent*

At a velocity equivalent to approximately Mach 2.0, deployment of the Viking heritage 19.7 m DGB supersonic parachute, Figure 3, is commanded. This parachute has a 49% larger reference area than the 16.15 m DGB parachute flown on Viking. However, the Planetary Entry Parachute Program successfully tested a similar 19.7 m DGB parachute at Mach 1.56 behind a 4.6 m aeroshell in a high altitude Earth test.

This paper will show that this parachute size is needed in order to decrease the on-chute ballistic coefficient, moving the system to match heritage values, while also providing improved altitude performance and reduced system sensitivities. In addition, the larger parachute size returns the ratio of parachute diameter to fore-body diameter back to Viking heritage values.

Once the parachute is deployed, the vehicle decelerates quickly through transonic to subsonic conditions. At this point, it is necessary to go through several reconfigurations in order to prepare for terminal powered descent. First the heatshield is removed. Then the balance mass is ejected to bring the center-of-gravity to the vehicle axis of symmetry. Then the Terminal Descent Sensor (TDS), or radar, is activated.

The first of these critical events, heatshield jettison, is required to occur at a Mach number less than 0.8 to ensure acceptable separation conditions through a ballistic coefficient difference driven by the relative aerodynamics of the heatshield and entry vehicle on parachute. The current system uses navigated velocity to trigger the heatshield separation event. The trigger set point is

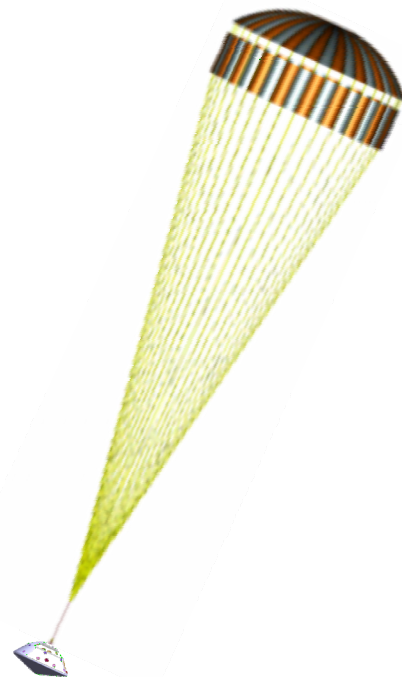


**Figure 3 – Disk-Gap-Band Parachute.**

*Sky Crane Maneuver and Rover Touchdown*

At a predetermined altitude, the rover is separated from the Descent Stage and lowered by the Bridle and Umbilical Descent Rate Limiter (BUD) at a constant velocity. A constant descent rate is continued until the terminal descent guidance senses rover touchdown.

*Descent Stage Flyaway and Impact*

Following touchdown, the bridle lines are separated from the rover and the Descent Stage executes a flyaway maneuver. Descent Stage flight is terminated by a hard encounter with the terrain at some distance from the landed rover.

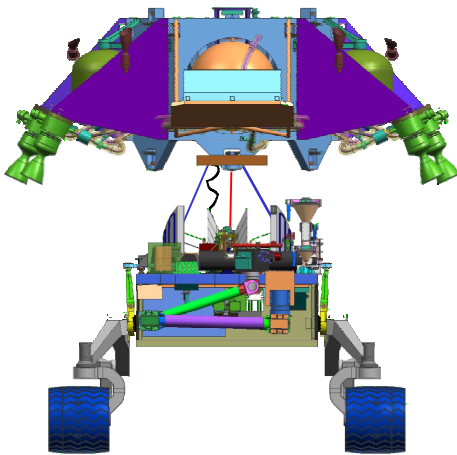


**Figure 4 – Sky Crane Configuration.**

### 3. MOTIVATION

The motivation for this paper is to understand a phenomenon observed in the MSL flight trajectory Monte Carlo simulations. In exploring a particular guided entry design option that resulted in an increase of 500 m in supersonic parachute deployment altitude, the heatshield jettison altitude was observed to increase by only 50 m. A tiger team investigation of the phenomena attributed the lower performance to an asymptotic approach to terminal velocity, and a work-around solution trade study was initiated. The central concern to the design team during this investigation was not just the obvious loss of performance, but also rather a concern about the increased sensitivity of the EDL design to assumptions of distributions in modeling inputs.

Between the July-2004 design and the June-2005 design, the rover mass increased 27% from 550 kg to 700 kg. This mass increase resulted in an entry mass allocation increase of 44% from 1883 kg to 2705 kg, as shown in Table 2 below. This mass growth raised the on-chute ballistic coefficient from 14 kg/m<sup>2</sup> to nearly 20 kg/m<sup>2</sup>. The result was a point design that met the EDL requirements, but was unacceptably sensitive to environmental modeling assumptions or additional mass growth.

**Table 2 – MSL Mass Growth**

Date	Rover Mass (kg)	Entry Mass (kg)	Ballistic Coefficient (kg/m <sup>2</sup> )	Parachute Diameter (m)
7/04	550	1883	13.6	16.15
12/04	600	2020	14.6	16.15
6/05	700	2705	19.5	16.15
12/05	775	2804	12.2	19.7

Many alternatives to correct this behavior were considered. However, increasing the parachute diameter to 19.7 m was the most direct solution, addressing the root cause of the problem, by lowering the on-chute ballistic coefficient back to 13 kg/m<sup>2</sup> and greatly improving the design sensitivities.

In addition, the larger parachute brings parachute geometric scaling back in family with Viking, maintaining the qualification heritage of the supersonic deployment and inflation tests conducted for that mission.

### 4. DEVELOPMENT

The observed asymptotic parachute performance sensitivity occurs at higher ballistic coefficients when the vehicle has insufficient drag acceleration due to close proximity to the terminal velocity asymptote. This condition occurs when the drag acceleration approaches the local gravitational acceleration, resulting in a small time rate of change of velocity.

Critical EDL events, such as heatshield jettison, are delayed, resulting in increased altitude loss. Observable

symptoms in EDL performance include decreased altitude performance and timeline margin, increased system sensitivities, diminishing returns associated with gains in supersonic parachute deploy altitude (compression factor), and lower landing site altitude capability.

$$\frac{dV}{dt} = g \cos \theta - \frac{q}{\beta} \quad \text{Equation 1}$$

Equation 1 is the time rate of change of velocity for an unpowered gravity turn. Drag (D) acting in the anti-velocity direction is assumed to be the only force acting on the vehicle. The local gravitational acceleration (g) acts at an angle ( $\theta$ ) from the velocity vector. Because shallow flight path angles are common in EDL, the off-vertical angle is not assumed to be small and no small angle approximation is taken.

$$\frac{D}{m} = \frac{qC_D A}{m} = \frac{q}{\beta} \quad \text{Equation 2}$$

In Equation 2, the drag acceleration (D/m) has been written in terms of the dynamic pressure (q) and the ballistic coefficient ( $\beta$ ). This form of the equation highlights the dependence on design parameters, such as entry mass and parachute size.

$$V_{term} = \sqrt{\frac{2\beta g \cos \theta}{\rho}} \quad \text{Equation 3}$$

The terminal velocity, Equation 3, is found by expanding the dynamic pressure (q) and solving for the velocity that results in zero acceleration. It can be seen from inspection that terminal velocity is not a constant since ballistic coefficient, dynamic pressure, and off-vertical angle are dependent on time, altitude, and velocity. Factors that increase the vehicle terminal velocity are increasing ballistic coefficient, steeper flight path angle, and decreasing atmospheric density.

$$\left( \frac{V}{V_{term}} \right) = \sqrt{\frac{q}{\beta g \cos \theta}} \quad \text{Equation 4}$$

Dividing the terminal velocity in Equation 3 by the actual velocity and inverting, results in Equation 4. This ratio (V/V<sub>term</sub>) is the percent of terminal velocity. Factors that improve the V/V<sub>term</sub> are increased dynamic pressure, lower ballistic coefficient, or a shallower flightpath angle (larger  $\theta$ ). V/V<sub>term</sub> is an indicator of system susceptibility to the asymptotic behavior previously discussed. Experience obtained from this analysis shows that the V/V<sub>term</sub> should be maintained above 1.5 to ensure sufficient drag deceleration.

## 5. SIMULATION RESULTS

The following simulation results illustrate the performance loss associated with increased on-chute ballistic coefficients and provide insight into the MSL EDL system behavior. These figures are taken from various MSL EDL flight trajectory Monte Carlo analyses, leading up to the MSL December 2005 baseline design. This MSL design is characterized by a 4.50 m aeroshell diameter, 2804 kg entry mass, 0.24 lift-to-drag ratio, and a single 19.7 m diameter supersonic parachute.

In constructing Figure 5, the nominal June 2005 MSL flight trajectory simulation was analyzed and the parachute deploy conditions were captured. Then sixteen additional simulations were run from the point of parachute deploy to heatshield jettison, while changing only the initial altitude of parachute deploy and the size of the supersonic parachute. Parachute deploy altitudes were varied from 10 to 16 km. On-chute ballistic coefficients were varied from 10 to 20 kg/m<sup>2</sup>. The heatshield jettison was triggered on an actual planet relative velocity equivalent to Mach 0.72. Figure 5 shows the resulting heatshield jettison conditions in altitude and off-vertical angle.

The dashed red lines of constant supersonic parachute deploy altitude show reduced heatshield jettison altitude with increasing on-chute ballistic coefficient, as expected. The solid blue lines of constant ballistic coefficient show the sensitivity of the heatshield jettison altitude with increasing supersonic parachute deploy altitude for the different ballistic coefficients. The lower ballistic coefficients (10 kg/m<sup>2</sup>) show a steep slope, which indicates a large percentage of the supersonic parachute deploy altitude gain is being realized at heatshield jettison (low altitude compression). However, the higher ballistic coefficients show shallower curves, which indicate less of the altitude gain is being realized at heatshield jettison (high altitude compression). At the highest ballistic coefficient (20 kg/m<sup>2</sup>) Figure 5 indicates that increasing the supersonic parachute deploy altitude from 14 to 16 km actually results in a lower heatshield jettison altitude.

The diminished return on supersonic parachute deploy altitude at higher ballistic coefficients, as seen by the shallower slope of the constant ballistic coefficient curves,

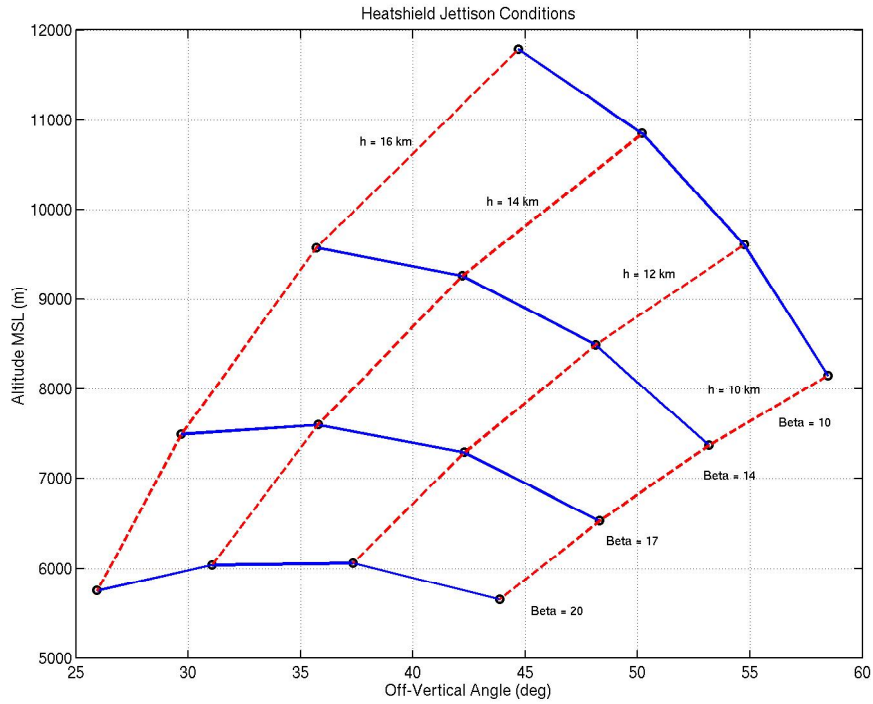


Figure 5 – HS Jettison Altitude for Various Ballistic Coefficients and SSP Deploy Altitudes.

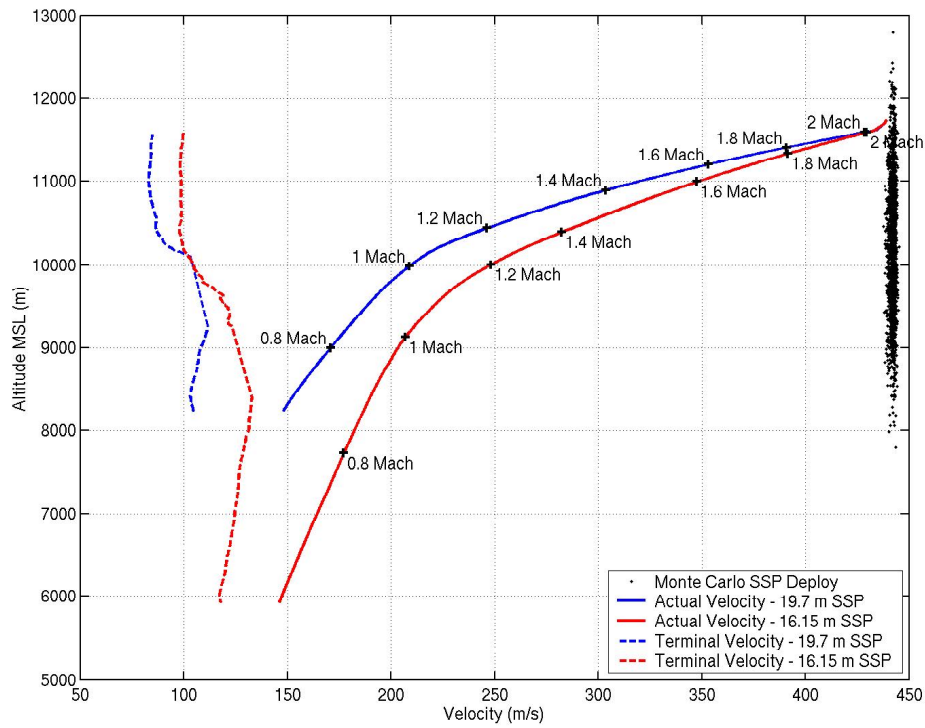


Figure 6 – Ballistic Coefficient Effect on Altitude Loss and Terminal Velocity

Figure 6 shows the altitude-velocity scatter plot of supersonic parachute deploy points from an MSL Monte Carlo analyses. The altitude-velocity trace from parachute deploy to heatshield jettison is shown for the Monte Carlo case with the steepest flight path angle at supersonic parachute deploy. Both actual velocities (solid curves) and terminal velocities, as calculated by Equation 3, (dashed curves) are shown for this case as a function of altitude. The blue curves are for a 19.7 m parachute. The red curves are for a 16.15 m parachute.

This figure highlights the drastic loss of attitude associated with the asymptotic approach to terminal velocity. The red curve (smaller parachute) has a larger ballistic coefficient and therefore a higher terminal velocity. The reduced  $V/V_{term}$  results in lower drag acceleration and increased altitude loss between supersonic parachute deploy and heatshield jettison. Additionally, this plot shows that the reduced ballistic coefficient associated with the 19.7 m SSP has resulted in over 2 km of altitude improvement over the 16.15 m parachute and approximately 20 seconds of timeline, at a 100 m/s terminal velocity, for identical SSP deploy conditions.

Figure 7 shows results from twelve Monte Carlo simulations. These Monte Carlo simulations were completed with various parachute sizes ranging in diameter from 16.15 to 19.7 m. The Monte Carlo analyses were run in pairs to examine an entry guidance design trade between improving altitude performance by commanding full lift-up near the equilibrium glide boundary versus reducing cross-

range delivery error in the normal heading alignment phase.

For each Monte Carlo pair with identical parachute size, the altitude gain at supersonic parachute deploy (approximately 500 m) is compared to the altitude gain at heatshield jettison. The altitude compression factor is defined as the ratio of SSP deploy altitude gain to the realized gain at heatshield jettison, and is plotted as a function of supersonic parachute diameter. An infinite compression ratio would indicate that none of the 500 m supersonic parachute deploy altitude gain was realized at heatshield jettison. Figure 7 depicted very graphically that the June 2004 MSL design (16.15 m parachute) was sitting very near an asymptote in performance and that a larger parachute would reduce the overall EDL system sensitivity to this phenomena.

Figure 8 shows collected results from twenty-four MSL Monte Carlo simulations. This figure investigates the sensitivity of heatshield jettison altitude to navigated velocity error under a wide range of initial attitude error assumptions. The red curves are for the smaller 16.15 m parachute and the magenta curves are for the larger 19.7 m parachute.

This plot shows that heatshield jettison altitude is very sensitive to navigation error resulting from initial attitude errors at Cruise Stage separation. The mechanism for this sensitivity is that in the presence of a positive velocity error (navigated velocity is higher than the actual velocity), the heatshield is jettisoned late (at a lower actual velocity and therefore lower altitude), when the navigated velocity

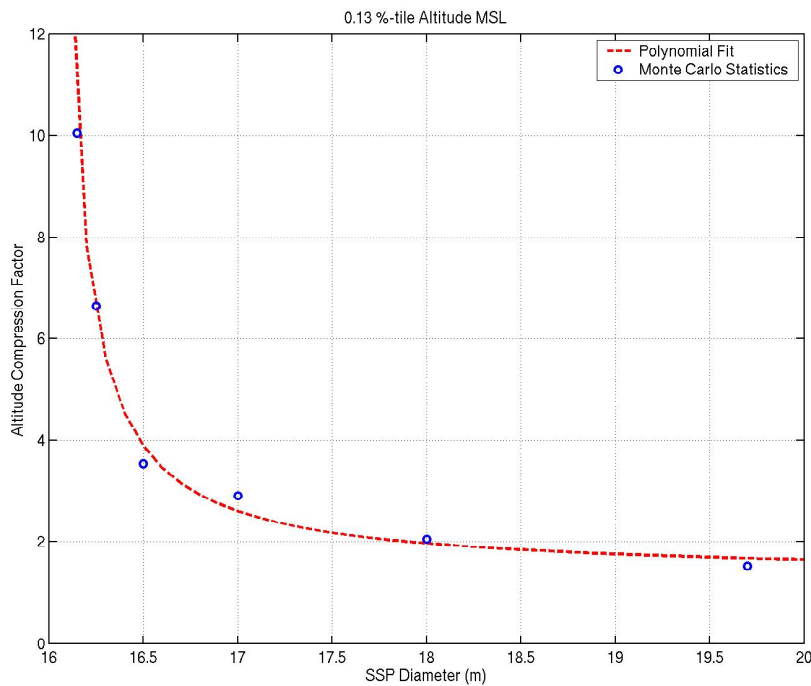


**Figure 7 – Altitude Compression vs. Parachute Size**



lowering the on-chute ballistic coefficient back to 13 kg/m<sup>2</sup> and greatly improving the design sensitivities. Experience obtained from this analysis shows that the ratio of velocity to terminal velocity should be maintained above 1.5 to ensure sufficient drag deceleration.

### **ACKNOWLEDGEMENTS**

The work described in this paper was carried out by the Jet Propulsion Laboratory, California Institute of Technology (under a contract with NASA) and the NASA Langley Research Center. The authors would like to recognize the contributions of the entire EDL design team members from JPL, JSC, ARC, and LaRC.

### **REFERENCES**

- [1] Golombek, M.P. et al., "Selection of the Mars Exploration Rover landing sites", *Journal of Geophysical Research*, Volume 108, Issue E12, pp. ROV 13-1, 2003.
- [2] Steltzner, A.D., Kipp, D.M., Chen, A., Burkhart, P.D., Guernsey, C.S., Mendeck, G.F., Mitcheltree, R.A., Powell, R.W., Rivellini, T.P., San Martin, A.M., Way, D.W., "Mars Science Laboratory Entry, Descent, and Landing System", IEEAC #1497, IEEE Aerospace Conference, March 4-11, 2006, Big Sky, MT.
- [3] Mendeck, G.F. and Carman, G.L., "Guidance Design for Mars Smart Landers Using The Entry Terminal Point Controller", AIAA-2002-4502 AIAA Atmospheric Flight Mechanics Conference and Exhibit, Monterey, California, Aug. 5-8, 2002.

### **BIOGRAPHY**

*David Way holds a BS from the United States Naval Academy, a MS from the Georgia Institute of Technology, and a PhD from the Georgia Institute of Technology. David joined NASA in 2002.*